

# BIOMASS REACTIVITY IN GASIFICATION BY THE HYNOL PROCESS

Yuanji Dong  
Acurex Environmental Corporation  
4915 Prospectus Drive  
Durham, NC 27709

Robert H. Borgwardt  
U.S. Environmental Protection Agency  
National Risk Management Research Laboratory  
Air Pollution Prevention and Control Division  
Research Triangle Park, NC 27711

Keywords: biomass gasification; gasification kinetics; biomass-to-methanol.

## INTRODUCTION

Methanol has many advantages to be considered as an alternative fuel. About 75% of methanol production uses natural gas as feedstock. Use of biomass as feedstock to produce methanol is of current interest because it offers substantial benefits for reduction of greenhouse gas emissions. The research and development of biomass-to-methanol processes, one of which is called Hynol, are now in progress.

The Hynol process was proposed to utilize biomass as a feedstock and natural gas as a cofeedstock to increase methanol yield and reduce costs (Steinberg and Dong, 1994). The process consists of three reaction steps: (1) gasification of biomass with the  $H_2$ -rich gas recycled from methanol synthesis, (2) steam reforming of the produced gas with an addition of natural gas feedstock, and (3) methanol synthesis from the  $H_2$  and CO produced by the reformer. A schematic flow diagram of the process is shown in Figure 1. Since the reaction of biomass with the  $H_2$  in the recycle gas to form  $CH_4$  is exothermic, the heat so generated is able to offset the energy required for other endothermic reactions in a Hynol gasifier. As a result, no expensive  $O_2$  plant or external heat source is needed for gasification. The use of natural gas as cofeedstock eases the requirement for a consistent composition of biomass feedstock. The integrated cyclical process configuration helps ensure the completion of overall conversion and increases thermal efficiency. CO shifting is not necessary and the requirement for acid gas removal is reduced, which lowers capital and operating costs.

A theoretical evaluation of the Hynol process conducted by the Air Pollution Prevention and Control Division (APPCD) of the National Risk Management Research Laboratory, U.S. Environmental Protection Agency (EPA), showed that the Hynol process represents a promising technology for maximizing fuel production inexpensively and with minimum greenhouse gas emissions (Borgwardt, 1995). Consequently, the APPCD established a laboratory to further assess the process feasibility. In the first phase of the study, a thermobalance reactor (TBR) was installed and used to evaluate biomass reactivity in gasification at the operating pressure, temperature, and feed gas composition specific for the Hynol process. The experimental work also attempted to improve understanding of the variables affecting Hynol gasification and identify needs for process development. This article summarizes the TBR results.

## EXPERIMENTAL

A flow diagram of the TBR system is detailed in Figure 2. The reactor is electrically heated and consists of a 35-mm I.D. stainless steel reactor pipe, a 305-mm O.D. pressure vessel, and a topwork which accommodates a weight transducer for measurement of sample weight during reaction. A pulley assembly is used to raise and lower a sample basket between the topwork and the reaction zone.

To initiate an experimental run, a basket with known weight of biomass sample was placed into the topwork through the removable window. A constant helium flow was introduced to the topwork to protect the wood sample from contact with process gas prior to entry in the reaction zone. Mass flow controllers were used to control the flow rates of  $H_2$ ,  $CH_4$ , CO, and  $CO_2$  from individual gas cylinders to obtain the desired feed gas composition. Steam was added to the feed gas from a steam generator fed with distilled water by a metering pump. The gas mixture was further heated by a superheater and then entered the reactor. The reactor exit gas was cooled in a condenser to remove moisture, and then depressurized through a back-pressure regulator before it was vented to atmosphere. When pressure and temperature in the reactor system were stabilized at the desired levels, the sample basket was lowered into the reaction zone and the change in sample

weight was automatically recorded by the transducer as a function of reaction time. A computer was used to control the TBR system and log experimental data. After gasification, the basket was raised back into the topwork and the reactor was depressurized and cooled. The discharged char was then weighed to determine the final sample weight. Because changes in gas composition across the sample are negligible, the reaction can be considered to take place at constant operating conditions.

In this study, the Hynol feed gas refers to a composition --  $H_2 = 65.83\%$ ;  $CH_4 = 11.63\%$ ;  $CO = 8.95\%$ ;  $CO_2 = 2.32\%$  and steam =  $11.27\%$  -- which is based on the results of a Hynol process simulation. Poplar wood, which is considered a primary candidate for large scale production as an energy crop for fossil fuel displacement (Wright, 1995), was used as a representative biomass sample. It was grown in North Carolina and cut to desired sizes and dried before its use. Composition is presented in Table 1.

## KINETIC MODEL AND DATA TREATMENT

The weight transducer output was recorded as a function of reaction time during a test. The records were converted into the data of variation in sample weight with time. The biomass conversion,  $X$ , on an ash-free basis was then calculated by :

$$X = \frac{W_0 - W}{W_0 - W_0 C_A} \quad (1)$$

where  $W_0$  is the initial sample weight,  $W$  is the sample weight at any reaction time,  $C_A$  is the weight fraction of ash obtained from the ultimate analysis of the original sample, and  $X$  is thus also a function of reaction time.

General observation of the reaction behavior revealed that biomass gasification under Hynol conditions involves two types of reactions: a rapid reaction, which may complete in a few seconds, involving devolatilization and pyrolysis reaction of the volatile matter in biomass with  $H_2$  and steam; and a very slow reaction of residual carbon with the process gas which requires hours to finish. To quantitatively describe the rate of gasification, these two reactions are assumed to be first order with respect to the remaining solid reactants. The rate of the rapid reaction can be expressed as:

$$\frac{dX_1}{dt} = k_1 (X_C - X_1) \quad (2)$$

and the rate expression for the slow reaction is:

$$\frac{dX_2}{dt} = k_2 (1 - X_C - X_2) \quad (3)$$

where  $X_1$  and  $X_2$  are the conversions by the rapid and slow reactions at time  $t$ ,  $X_C$  is the maximum attainable conversion by the rapid reaction, and  $k_1$  and  $k_2$  are the reaction rate constants for the rapid reaction and the slow reaction, respectively.

By integrating Equations (2) and (3), the total biomass conversion can be expressed by:

$$X = X_1 + X_2 = 1 - X_C \exp(-k_1 t) - (1 - X_C) \exp(-k_2 t) \quad (4)$$

The model involves three parameters:  $X_C$ ,  $k_1$ , and  $k_2$ , which are functions of operating conditions such as biomass properties, reaction temperature, pressure, and feed gas composition. They can be determined by fitting Equation (4) to the experimental conversion data obtained from TBR tests.

## RESULTS AND DISCUSSIONS

The above model was used to correlate the experimental data obtained from TBR tests. Figure 3 is a typical example of curve fitting results by the model, showing good agreement between the experimental data and the model regression over the entire reaction period.

Four different sizes of poplar particles were used to investigate the effects on gasification: 7/16-in diameter cylinders, 1/4-in diameter cylinders, 1/8-in cubes, and 20 to 30 mesh sawdust. The

rate of the rapid reaction increased significantly as a result of higher heat transfer and intraparticle diffusion rates when particle size was reduced from 7/16- to 1/8-in. Agglomeration during gasification was observed for the particles larger than 1/8-in, which inhibited gas diffusion within the particles. Sawdust heated up more quickly, and no agglomeration was observed. Experimental results showed that, at 30 atm and 800°C, about 87% of the 1/8-in poplar particles and 90% of the sawdust can be gasified by the Hynol feed gas in 60 min.

The analysis of the charred samples obtained from 7/16-in poplar particles showed that some of the volatile matter remains after gasification. However, for 1/8-in poplar particles or sawdust, nearly all of the H and O were converted into product gas in 20 min.

The agglomerates of residual chars formed in the TBR were fragile. If a fluidized bed gasifier is used, agglomeration is not likely to occur as a result of attrition; therefore, higher reaction rate and conversion than observed in TBR testing are expected in such systems.

The rapid-reaction stage of poplar gasification was found to be essentially completed in less than 0.2 to 0.3 min, contributing most of the biomass conversion. A small additional conversion is contributed by the slow reaction. To achieve high biomass conversion, sufficient gasification time must be provided. Tests showed that biomass conversion increased from 85 to 90% when gasification time extended from 20 to 150 min. The comparison between the compositions of chars after 20 and 150 min gasification indicated that there was virtually no further conversion of H and O in the char after 20 min and that the additional conversion resulted from the reaction of carbon with the process gas.

Experimental results of 60-min gasification with sawdust and 1/8-in poplar particles at different reaction temperatures showed great increase in biomass conversion and gasification rates when temperature increased from 750 to 950°C as shown in Figure 4. The rate constants for the rapid and slow reactions,  $k_1$  and  $k_2$ , at different reaction temperatures were determined by fitting the experimental data for gasification of 1/8-in poplar particles. The rate constants thus obtained were plotted against the reciprocal of the absolute temperature, as shown in Figure 5, and expressed as functions of reaction temperature by the Arrhenius equation:

$$k_i = k_{i0} \exp\left(-\frac{E_i}{RT}\right) \quad (5)$$

where subscript  $i$  is 1 for the rapid reaction and 2 for the slow reaction.  $E_i$  is the activation energy. The results obtained were:  $k_{10} = 108.85 \text{ min}^{-1}$ ,  $E_1 = 3.78 \text{ kcal/mol}$ ,  $k_{20} = 22925 \text{ min}^{-1}$ , and  $E_2 = 34.1 \text{ kcal/mol}$ . The maximum attainable conversion by the rapid reaction,  $X_C$ , was also correlated as a function of temperature for gasification of 1/8-in poplar particles by:

$$X_C = 0.9611 - 0.000149T \quad (6)$$

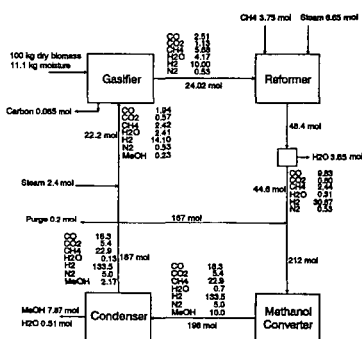
where  $T$  is the reaction temperature in °C. With Equations (4), (5), and (6) and the values of  $k_{10}$ ,  $E_1$ ,  $k_{20}$ , and  $E_2$ , the conversions of 1/8-in poplar particles at different temperatures and gasification times were predicted. Figure 6 compares the prediction with the conversion data obtained from the separate experimental tests at different temperatures and gasification times. The comparison covers a temperature range of 750 to 950°C and a gasification time range from 0.2 to 150 min for 1/8-in poplar particles gasified by the Hynol feed gas at 30 atm. The activation energy obtained for the rapid reaction was low, implying that heat transfer dominates the rates of devolatilization and pyrolysis of biomass in the TBR.

The effect of feed gas composition on poplar gasification was investigated by varying the flow rates of individual gas components under constant system pressure. Helium was used as an inert "make-up" gas for this purpose. At 30 atm and 800°C, the final conversion of poplar wood gasified by pure helium after 60 min was about 6% lower than that obtained under pure  $H_2$ . If the conversion obtained after 60 min of gasification is plotted against  $H_2$  partial pressure ( $P_{H_2}$ ), a linear relationship,  $\text{conversion} = 0.0017 \times P_{H_2}$ , was found. When steam partial pressure in the feed gas was varied from 7 atm to zero while the partial pressures of other gas components remained constant, the conversion was proportional to steam partial pressure or  $0.003 \times P_{H_2O}$ . Negligible effects on the gasification conversion and reaction rate of 1/8-in poplar particles were observed as the  $CH_4$  in the feed gas was reduced from the simulated Hynol composition, 11.63%, to zero. Replacing CO and  $CO_2$  in the feed gas with helium did not affect the gasification rate. The conversion and reaction rates of 1/8-in poplar particles gasified by the Hynol feed gas were nearly the same as those observed by the feed gas containing no CO and  $CO_2$ .

Borgwardt, R. (1995): The Hynol Process, Presented at Symposium on Greenhouse Gas Emissions and Mitigation Research, Washington, DC. June 27-29.

Wright, L. (1995): Demonstration and Commercial Production of Biomass for Energy, Proceedings, Second Biomass Conference of the Americas, NREL/CP-200-8098, National Renewable Energy Laboratory, Golden, CO, pp. 1-10.

Carbon (wt.%)	51.52	Volatile (wt.%)	91.38
Hydrogen (wt.%)	6.20	Fixed carbon (wt.%)	8.15
Oxygen (wt.%)	41.37		
Ash (wt.%)	0.47	Higher heating value	
Sulfur (wt.%)	0.02	(Btu/lb dry wood)	8768.
Nitrogen (wt.%)	0.42		



The schematic diagram illustrates the gas analysis system for the thermobalance reactor. Gases H<sub>2</sub>, CH<sub>4</sub>, CO, and CO<sub>2</sub> are introduced into the system from the left. These gases pass through a series of components: a 'Heat Tracing #1' unit, a 'Stream' (likely a water trap or separator), and another 'Heat Tracing #2' unit. The gas then enters the 'Thermobalance Reactor', which is a vertical cylindrical vessel. Above the reactor is a 'Condenser' and below it is a 'Superheater'. The gas exits the reactor through a 'Back-Pressure Regulator' and a 'Trap' before entering a 'Dry Gas Meter'. The final output is labeled 'Vent'.

1348

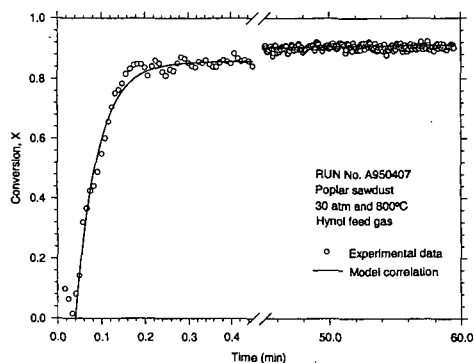


Figure 3. Example of TBR experimental data fitting by the model.

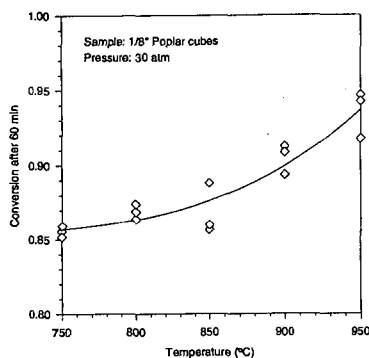


Figure 4. Effect of reaction temperature.

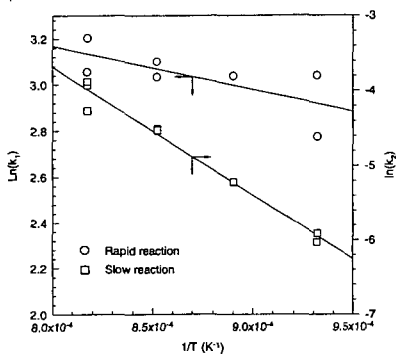


Figure 5. Arrhenius plots of the rate constants.

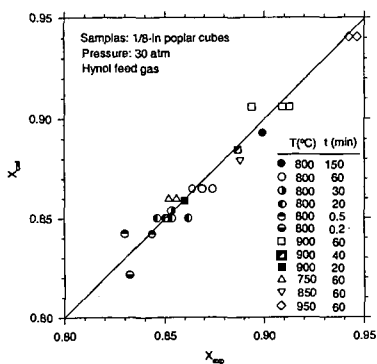


Figure 6. Comparison of the model prediction with experimental conversion data.